Modeling, Identification and Control, Vol. 37, No. 1, 2016, pp. 41–52, ISSN 1890–1328

Model-Free Predictive Anti-Slug Control of a Well-Pipeline-Riser.

Christer Dalen [1] David Di Ruscio [2]

[1] *Skien, Norway. E-mail:* christerdalen@hotmail.com

[2] *University College of Southeast Norway, P.O. Box 203, N-3901 Porsgrunn, Norway. E-mail:* david.di.ruscio@hit.no

Abstract

Simplified linearized discrete time dynamic state space models are developed for a 3-phase well-pipeline-riser and tested together with a high fidelity dynamic model built in K-Spice and LedaFlow. In addition the Meglio pipeline-riser model is used as an example process. These models are developed from a subspace algorithm, i.e. Deterministic and Stochastic system identification and Realization (DSR), and implemented in a Model Predictive Controller (MPC) for stabilizing the slugging regime. The MPC, LQR and PI control strategies are tested.

Keywords: Model-Free, Model Predictive Control, Kalman filter, system identification, anti-slug, well-pipeline-riser

1. Introduction

Severe-slugging is a problem regarding well-pipeline-riser processes in the offshore industry and is characterized by significant flow rate and pressure oscillations observed at the topside choke. This flow needs to be stabilized or it might damage both downstream equipment and personnel (Courbot (1996)).

One solution, which is regarded as the most cost-effective, is to introduce active feedback where we define the topside choke valve as the manipulative variable and some pressure, flow rate or density measurements as the controlling variable. We may also define the flow rate as the goal variable, as it is what we want to maximize.

On this approach, Schmidt Z. (1979), may be viewed as the first contribution, however this was a rather experimental approach where an upstream pressure measurement together with the flow rate measurement, the choke valve was automatically changed, by algorithm, to counteract the slugging regime.

To maximize the goal variable a controller needs to be designed to operate around an open-loop unstable working point, here the largest possible choke opening which stabilizes the system may be defined as a performance measure of the controller.

Model-based control using mechanistic models is a popular approach for designing controllers. Some of these mechanistic models are presented in Storkaas and Skogestad (2003b), Di Meglio et al. (2009), Jahanshahi and Skogestad (2013) and compared in Jahanshahi and Skogestad (2013).

Several active control strategies have been addressed for stabilizing the slugging phenomena, some of them are mentioned in Godhavn et al. (2005), Ogazi AI (2010), Di Meglio et al. (2010a), Storkaas and Skogestad (2003a) and Jahanshahi and Skogestad (2015), Dalen et al. (2015).

In Dalen et al. (2015), a so called Model-Free Linear-Quadratic Regulator (MFLQR) was demonstrated on a well-pipeline-riser example integrated in the K-Spice/LedaFlow simulator (K-Spice, LedaFlow). Different input-output cases were considered for solving the slugging problem, where the most satisfying results were when introducing gas-lift, however this is a rather expensive solution, as large quantities of gas are needed. It is less expensive to stabilize the flow regime, or controlling the bottom riser pressure, by active choking of the topside choke valve also demonstrated in the paper.

The concept of model free optimal control is not new and was used in Favoreel et al. (1999) in order to identify a Linear-Quadratic-Gaussian (LQG) controller directly from closed loop subspace system identification. The subspace method used was however/regardless biased and the controller has to be partly known.

In this paper we will define bottom-riser pressure as the controlling variable and topside choke valve as the manipulative variable. In particular, demonstrations of Model-Free Predictive Control (MFPC) is performed on the 3 state Di Meglio model (Di Meglio et al. (2009)) and on the K-Spice/LedaFlow simulator (K-Spice, LedaFlow).

The contributions of this paper can be itemized as follows.

- MFPC and MFLQR of the Di Meglio model (Di Meglio et al. (2009)).
- MFPC of the K-Spice/LedaFlow simulator.

The rest of the paper is organized as follows. In Sec. 2 we define the MFPC algorithm. In Sec. 3 we present results of the MFPC algorithm on the Di Meglio model (Di Meglio et al. (2009)) and the K-Spice/LedaFlow simulator. In Sec. 4 we discuss and summarize the results. In Sec. 5 we present the concluding remarks. In Appendix A we provide a complete model description of the Di Meglio model (Di Meglio et al. (2009)).

2. Theory

Definition 2.1 (State observer)
Define the following Kalman filter on state deviation form, i.e.

$$\begin{aligned}\Delta\bar{x}_{k+1} &= A\Delta\bar{x}_k + B\Delta u_k + K(y_k - y_{k-1} - D\Delta\bar{x}_k),\\ \Delta\bar{x}_0 &= 0,\end{aligned} \tag{1}$$

where $k \in \mathbb{N}$ is the discrete time, $\Delta\bar{x}_k \in \mathbb{R}^n$ is the predicted state deviation vector, $\Delta u_k \in \mathbb{R}^r$ is the input deviation vector, $y_k \in \mathbb{R}^m$ is the output vector and K is the Kalman filter gain matrix. The observer matrices A, B, D, K are identified as in Eq. (2).

Definition 2.2 (Optimal model)
The model matrices in Eq. (1) are found using the following MATLAB function,

$$\begin{bmatrix} A & B & D & K \end{bmatrix} = dsr\_op(Y, U), \tag{2}$$

where Y and U are identification matrices, containing collected data from an experimental design.

$$Y = \begin{bmatrix} y_1^T \\ \vdots \\ y_N^T \end{bmatrix}, \quad U = \begin{bmatrix} u_1^T \\ \vdots \\ u_N^T \end{bmatrix}. \tag{3}$$

It is important to note that choosing the model based on lowest Mean Square Error (MSE), calculated from simulated output, as in Dalen et al. (2015), might not give the optimal model order, and according to Akaike (1974). The optimal model will be refereed to as DSR_L^J, where J is the past horizon and L is the future horizon (see Di Ruscio (1996) for a detailed description).

Definition 2.3 (MPC Algorithm)
We consider the simple MPC algorithm presented in Di Ruscio (2013).

Given the pre-defined matrices, $H, O_L\tilde{A}, F_L^T Q$, as defined in Di Ruscio (2013), and the reference matrix, $r_{k+1|L}$, we have for each time-instant k that

$$\begin{aligned}\tilde{x}_k &= \begin{bmatrix} \Delta\bar{x}_k \\ y_{k-1} \end{bmatrix},\\ p_L &= O_L\tilde{A}\tilde{x}_k,\\ f_k &= F_L^T Q(p_L - r_{k+1|L})\end{aligned} \tag{4}$$

The optimal unconstrained predictive control is

$$\Delta u^*_{k|L} = -H^{-1} f_k. \tag{5}$$

The actual control is

$$u_k = u_{k-1} + \Delta u^*_{k|1}. \tag{6}$$

However, if the constrains are active, the problem renders a general QP problem, i.e.

$$\Delta u^*_{k|L} = \arg \min_{\mathcal{A}\Delta u_{k|L} \leq b_k} J_k, \tag{7}$$

where

$$J_k = \Delta u_{k|L}^T H \Delta u_{k|L} + 2 f_k^T \Delta u_{k|L} + J_0, \tag{8}$$

and J_0 is not used. The vector b_k depends on the constraints.
As an example regarding the linear inequality in Eq. (7), we consider the input rate of change constraints,

$$\Delta u_{k|L}^{min} \leqslant \Delta u_{k|L} \leqslant \Delta u_{k|L}^{max}. \tag{9}$$

Eq. (9) may be expressed as $\mathcal{A}\Delta u_{k|L} \leq b_k$, where

$$\begin{aligned}\mathcal{A} &= \begin{bmatrix} I_{LrxLr} \\ -I \end{bmatrix},\\ b_k &= \begin{bmatrix} \Delta u_{k\|L}^{max} \\ -\Delta u_{k\|L}^{min} \end{bmatrix}.\end{aligned} \tag{10}$$

A complete example which introduces the constraints of both the input rate of change and the input amplitude can be found in Section 3.2 and Appendix A in Di Ruscio (2013).

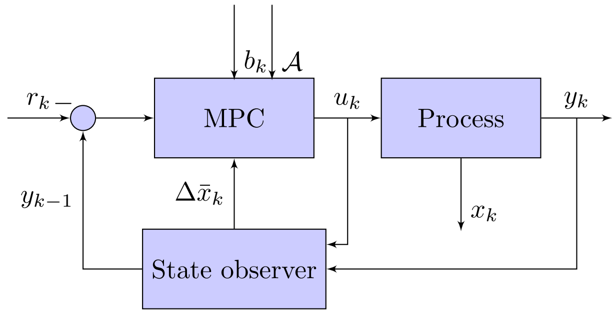

Figure 1: Block diagram illustrating MFPC.

3. Numerical Examples

3.1. Di Meglio model

We consider the 3 state model presented in Di Meglio et al. (2009), which was calibrated in Di Meglio et al. (2010b), for reproducing the slugging regime present in a real oil well located in the North Sea. The model is rather simple, but with an introduced virtual valve located at the bottom of the riser the model proves sufficient to investigate the physical aspects of the slugging phenomenon.

This model may be formulated as a continuous non-linear state space model, as

$$\begin{aligned} \dot{x} &= f(x, u), \\ y &= g(x), \end{aligned} \tag{11}$$

where

$$x = \begin{bmatrix} x_1 \\ x_2 \\ x_3 \end{bmatrix} = \begin{bmatrix} m_{g,cb} \\ m_{g,r} \\ m_{l,r} \end{bmatrix}. \tag{12}$$

Here, in Eq. (12), $m_{g,cb}$ is the mass of gas in the elongated bubble, $m_{g,r}$ is the mass of gas in the riser, $m_{l,r}$ is the mass of liquid in the riser and the output y is the pressure at the riser bottom. See Di Meglio et al. (2009) for details. The main control u is the topside choke. The complete model for direct implementation is presented in Appendix A with parameters as in Tab. 6.

The continuous non-linear model may be linearized around steady state operating points u^s and x^s, which leads to a discrete time linear model,

$$\begin{aligned} x_{k+1} &= Ax_k + Bu_k + v, \\ y_k &= Dx_k + w. \end{aligned} \tag{13}$$

Now, we present results on the MFPC based upon two different datasets with length, $N = 2000$ samples, each excited around different choke openings, @0.15 and @0.20, illustrated in Figs. 2 and 7, respectively. The sampling time is chosen equal to 100 sec.

We can define our two cases as

$$y \in \mathbb{R} := \Big\{ \text{Bottom-riser pressure, } [bar] \quad ,$$

$$u \in \mathbb{R} := \Big\{ \text{Topside choke @ } \{0.15, 0.20\} \ [1]$$

Note that $u > 0.205$ is considered the bifurcation point, i.e. the choke opening where the process becomes marginally stable.

We removed the first 200 samples. Now, the first 1301 were stored in input and output identification vectors $U \in \mathbb{R}^{N_{id}}$ and $Y \in \mathbb{R}^{N_{id}}$, respectively. The validation vectors were made from all the data, stored as $U \in \mathbb{R}^{N_v}$ and $Y \in \mathbb{R}^{N_v}$, illustrated in Fig. 2.

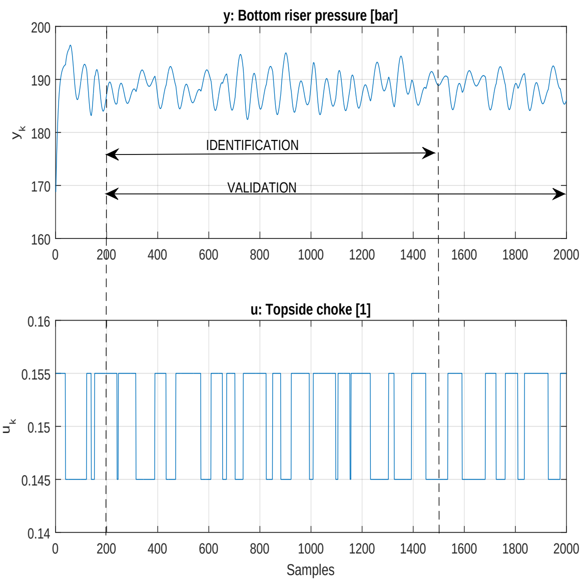

Figure 2: Raw data with length, $N = 2000$ samples. Identification and validation with lengths, $N_{id} = 1301$ and $N_v = 1800$. Sampling time is 100 sec. @0.15

The vectors U and Y were redefined with centered data, i.e. subtracted by the mean values $u_m = 0.151$ and $y_m = 188.3$ (Fig. 3).

Next, a 3rd order model was identified (Eq. 14) using *dsr_op* as in Eq. (2), and Eqs. (15) and (17) for

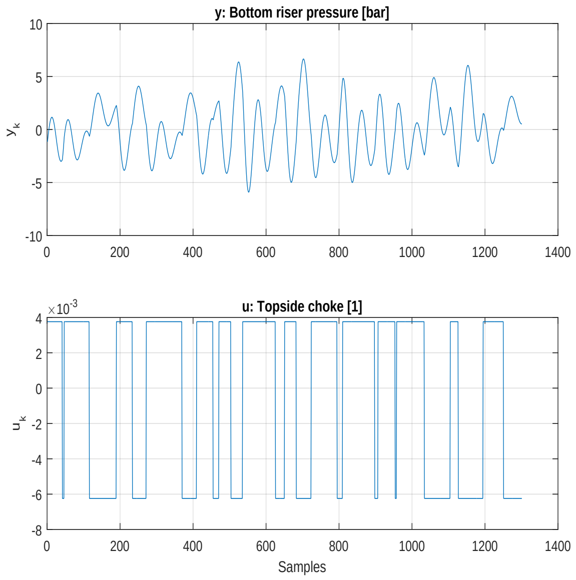

Figure 3: Identification data, $N_{id} = 1301$ samples. Sampling time is 100 sec. @0.15

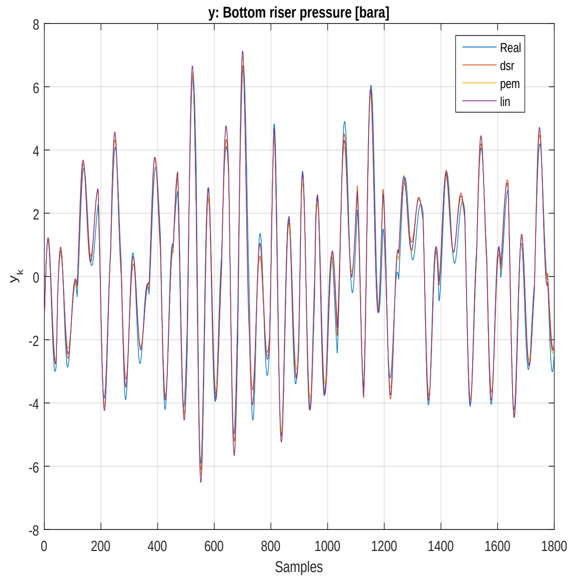

Figure 4: The identified models simulated and compared to validation data gathered from the real process (Di Meglio). We have the following validation performances (measured with MSE); $V_{DSR_3^9} = 0.1912$, $V_{PEM} = 0.2175$ and $V_{LIN} = 0.2182$.

an observability canonical form version of DSR_3^{12}, for @0.15 and @0.20 operating points, respectively. The original DSR_3^{12} is shown in Eq. (16). Fig. 4 shows three models; DSR_3^9, PEM and LIN, simulated over the validation data, where the best performing model was the dsr with $V_{DSR} = 0.1912$, $V_{PEM} = 0.2175$ and $V_{LIN} = 0.2182$ (See Tab. 1). A well-known algorithm in system identificaiton is the Prediction Error Method (PEM), which can be found in the system identication toolbox (Ljung (2007)).

$$\overbrace{\begin{aligned} A &= \begin{bmatrix} 0.9687 & 1.2029 & -1.3586 \\ -0.0115 & 0.9907 & -2.6130 \\ 0.0001 & -0.0001 & 0.5151 \end{bmatrix}, \\ B &= \begin{bmatrix} 48.6373 \\ 3.2090 \\ -0.3945 \end{bmatrix}, \\ D &= \begin{bmatrix} -0.5903 & 0.6984 & 0.4046 \end{bmatrix}, \\ K &= \begin{bmatrix} -5.6098 \\ -1.8145 \\ 0.0413 \end{bmatrix}. \end{aligned}}^{\textbf{Identified model: } DSR_3^9} \tag{14}$$

$$\overbrace{\begin{aligned} A &= \begin{bmatrix} 0.0000 & 1.0000 & 0.0000 \\ -0.0000 & 0.0000 & 1.0000 \\ 0.5012 & -1.9827 & 2.4745 \end{bmatrix}, \\ B &= \begin{bmatrix} -26.6303 \\ -27.9387 \\ -29.7707 \end{bmatrix}, \\ D &= \begin{bmatrix} 1.0000 & 0.0000 & 0.0000 \end{bmatrix}. \end{aligned}}^{\textbf{Observability canonical: } DSR_3^9} \tag{15}$$

Implementation of the MFPC is shown in Figs. 5 and 10. These figures shows how similar the LQR and MPC strategies are.

$$\overbrace{\begin{aligned} A &= \begin{bmatrix} 0.9823 & 0.8806 & -0.8337 \\ -0.0338 & 0.9836 & -2.0235 \\ 0.0000 & 0.0000 & 0.8481 \end{bmatrix}, \\ B &= \begin{bmatrix} 47.0290 \\ 4.6173 \\ -0.0688 \end{bmatrix}, \\ D &= \begin{bmatrix} -0.4944 & 0.6695 & 0.5089 \end{bmatrix}, \\ K &= \begin{bmatrix} -8.9128 \\ -3.3314 \\ 0.1692 \end{bmatrix}. \end{aligned}}^{\textbf{Identified model: } DSR_3^{12}} \tag{16}$$

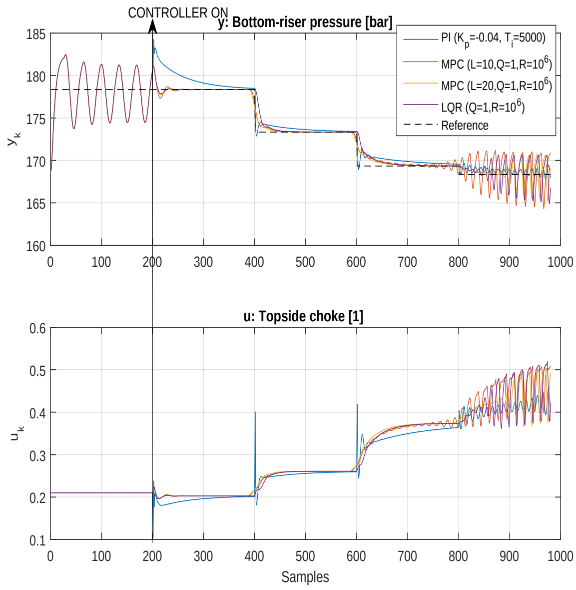

Figure 5: Four controllers, based @0.15, are implemented on the real process (Di Meglio) turned on from starting point $k = 200$. We are comparing LQR, MPC (L=10), MPC (L=20) and PI. The PI controller is tuned using MATLAB Tuner Application. The weights for MPC and LQR are chosen to be the same values. Sampling time is 100 sec.

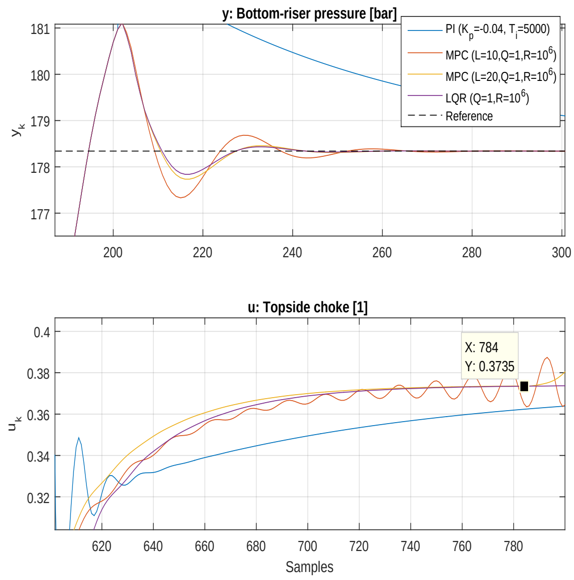

Figure 6: The subfigure above illustrates how the MPC converges to the LQR when the prediction horizon, L increases. The subfigure below illustrates the controller performances. MPC (L=20) and the LQR based @0.15 are able to stabilize the slugging regime up to choke opening 0.37 (zoomed in on the first and last part of Fig. 5.)

Table 1: Summary: Comparing models from DSR_L^J, PEM and Linearized (LIN). We have the prediction error for simulated output, V_{MSE}, the steady state gain, H_d, and absolute eigenvalues, $abs(eig(A))$, for each of linear models, Mod. @ means around working point.

MOD	@	V_{MOD}	H_d	abs(eig(A))
DSR_3^9	0.15	0.1912	-299.2	0.9874, 0.9874 0.5140
PEM	0.15	0.2175	-283.0	0.9864, 0.9864
LIN	0.15	0.2182	-289.1	0.9876, 0.9876 0.0000
DSR_3^{12}	0.20	0.0798	-126.8	0.9980, 0.9980 0.8481
PEM	0.20	0.1327	-122.1	0.9979, 0.9979 0.9625, 0.9625
LIN	0.20	0.1326	-131.6	0.9977, 0.9977 0.0000

Table 2: Summary: Comparing controllers PI, MPC and LQR by performance measures IAE and TV, calculated from $k = 200$ to $k = 800$. Maximum choke opening while stable is donated by max u. Measures donated by * should not be considered.

Cont.	@	Param.	IAE	TV	max u
PI	0.15	$K_p = -0.04$ $T_i = 5000$	448.1	1.44	0.37
MPC $L = 10$	0.15	$Q = 1$ $R = 10^6$	168.5 *	0.38*	0.26
MPC $L = 20$	0.15	$Q = 1$ $R = 10^6$	125.3	0.24	0.37
LQR	0.15	$Q = 1$ $R = 10^6$	167.6	0.23	0.37
PI	0.20	$K_p = -0.05$ $T_i = 6000$	442.6	1.12	0.39
MPC $L = 10$	0.20	$Q = 1$ $R = 10^6$	239.2*	0.71*	0.29
MPC $L = 20$	0.20	$Q = 1$ $R = 10^6$	134.6	0.27	0.39
LQR	0.20	$Q = 1$ $R = 10^6$	159.3	0.24	0.39

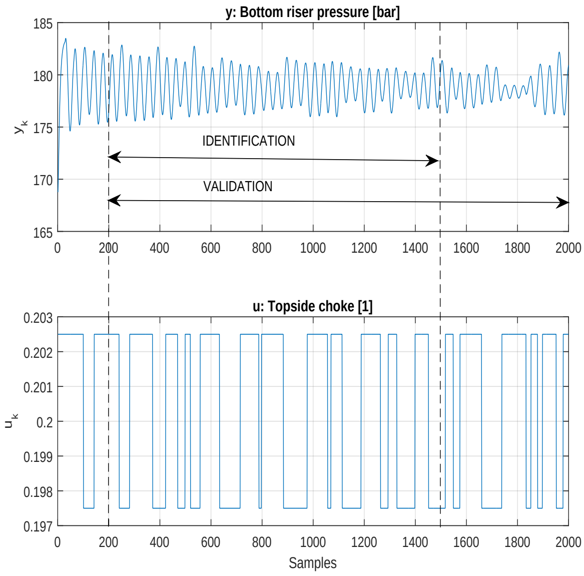

Figure 7: Raw data with length, $N = 2000$ samples. Identification and validation are chosen with lengths, $N_{id} = 1301$ and $N_v = 1800$. Sampling time, $\Delta t = 100$ sec. @0.20

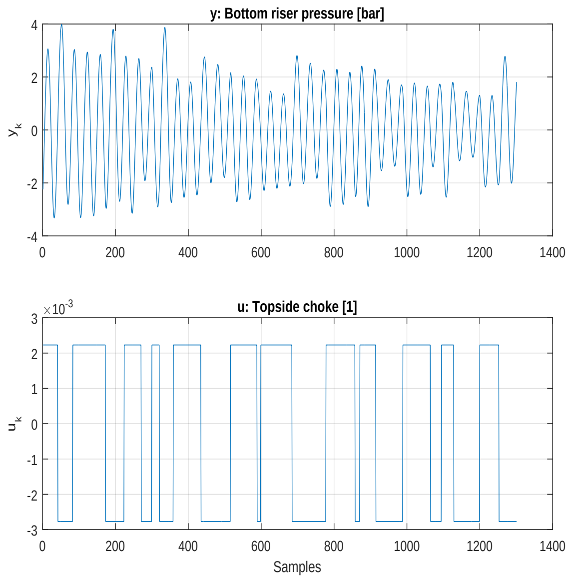

Figure 8: Identification data, $N_{id} = 1301$ samples. @0.20

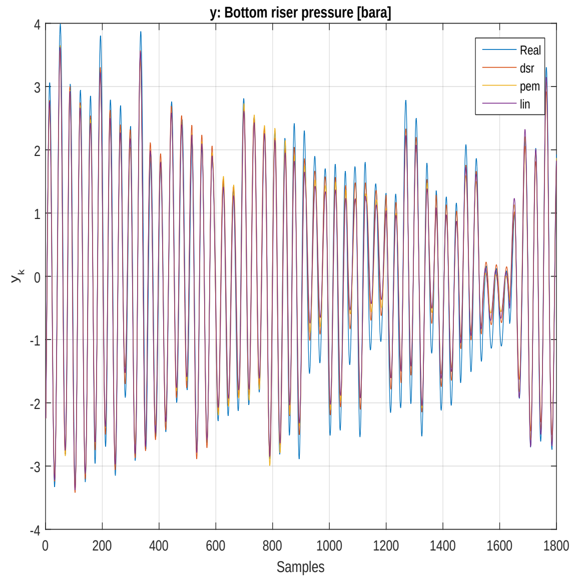

Figure 9: Identified dsr model simulated over the validation set. $V^{DSR_3^{12}} = 0.0862$. @0.20

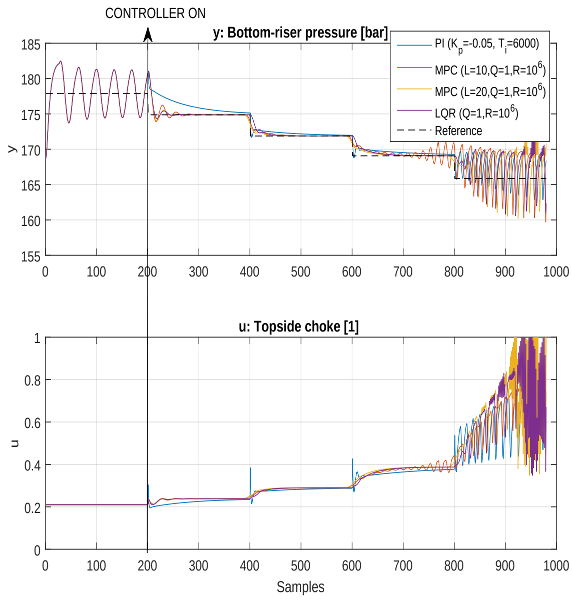

Figure 10: Four controllers, based @0.20, are implemented on the real process (Di Meglio), where each controller is turned on from starting point $k = 200$. We are comparing LQR, MPC (L=10), MPC (L=20) and PI. The PI controller is tuned using MATLAB Tuner Application. The weights for MPC and LQR are chosen the same values. Sampling time is 100 sec.

$$\overbrace{A = \begin{bmatrix} 0.0000 & 1.0000 & 0.0000 \\ 0.0000 & 0.0000 & 1.0000 \\ 0.8447 & -2.6632 & 2.8139 \end{bmatrix},}^{\textbf{Observability canonical: } DSR_3^{12}} \quad B = \begin{bmatrix} -20.1942 \\ -22.8393 \\ -24.8593 \end{bmatrix}, \quad D = \begin{bmatrix} 1.0000 & 0.0000 & 0.0000 \end{bmatrix}. \tag{17}$$

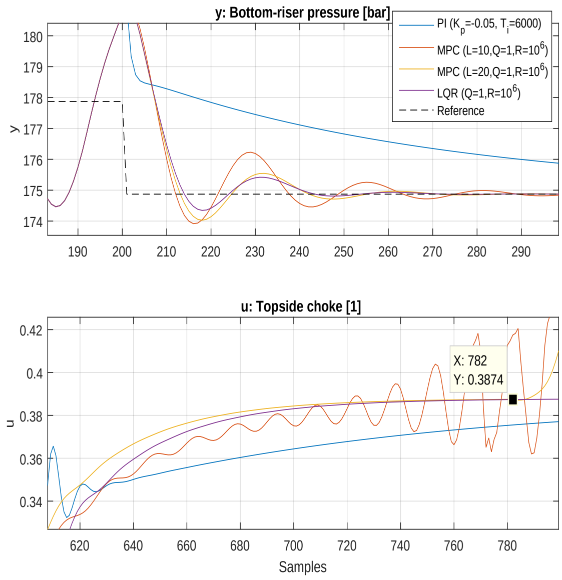

Figure 11: The subfigure above illustrates how the MPC converges to the LQR when the prediction horizon, L increases. The subfigure below illustrates the controller performances. The MPC (L=20) and the LQR, based @0.20, are able to stabilize the slugging regime up to choke opening 0.39. (zoomed in on the first and last part of Fig. 10.

3.1.1. Discussion

Interestingly, considering Tab. 1 , the dsr model is performing better than the PEM and the linearized model in both cases; 0.15 and 0.20.

Considering Tab. 2 the best performing controller seems to be MPC(L=20) based at @0.20, stabilizing up to 0.39. However, MPC(L=20) based at 0.15 is surprisingly achieving stabilizing up to 0.37. The LQR seems to be the runner-up best candidate.

3.2. The K-Spice/LedaFlow simulator

We perform model-free anti-slug control on a well-pipeline-riser (Fig. 12), integrated in the K-Spice/LedaFlow simulator, high fidelity simulators developed by Kongsberg Oil & Gas Technologies (K-Spice, LedaFlow).

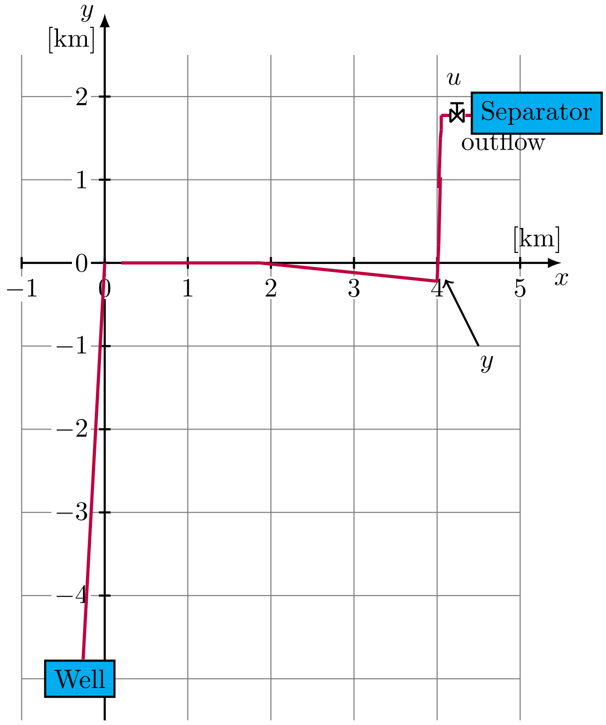

Figure 12: Illustration of the 3-phase well-pipeline-riser process integrated in the K-Spice/LedaFlow simulator.

We define following case as

$$y \in \mathbb{R} := \left\{ y\text{: Bottom-riser pressure } [bara] \right. ,$$
$$u \in \mathbb{R} := \left\{ u\text{: Topside choke } [\%] \right. .$$

Note that bara is the absolute pressure expressed in bar, where 0 bara is associated with total vacuum.

The simulator was run with simulation speed 50 times real-time and the sample time was chosen to be 1 sec. Input and output data were collected from an open loop input experiment (Fig. 13). The samples from 600 to 2000 were stored in identification matrices $U \in \mathbb{R}^N$ and $Y \in \mathbb{R}^N$, where $N = 1400$. The samples from 600 to 2350 were stored in validation matrices. The matrices were redefined with centered data, i.e. subtracted by mean values $u_m = 44.9$ and $y_m = 58.3$.

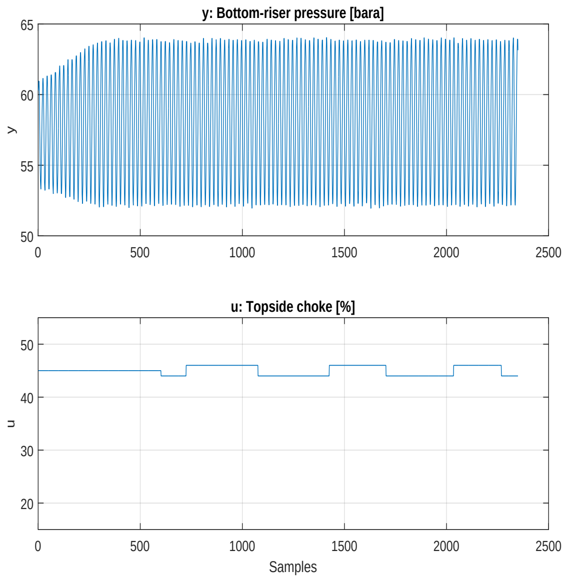

Figure 13: Data collected from the K-Spice/LedaFlow simulator. The data from 600 to 2000 Samples were used for identification, while the data from 600 to 2350 were used for validation. The simulation speed was 50 times real-time. The sampling time is equal to 1 sec.

An optimal model was identified (Eq. 18), i.e. the model from DSR_L^J having the lowest prediction error using deterministic output (as described in Eqs. (9)-(10) in Dalen et al. (2015)) with $L = J = 8$, $n = 4$ and resulting in $V_{MSE} = 0.3753$. See Fig. 14 for illustration.

$$\overbrace{\begin{aligned} A &= \begin{bmatrix} 0.9560 & 0.3942 & -0.1276 & -0.3756 \\ -0.2238 & 0.9488 & -0.7297 & -0.4976 \\ 0.0006 & 0.0048 & 0.8530 & 1.4303 \\ 0.0008 & -0.0013 & -0.2119 & 0.7922 \end{bmatrix}, \end{aligned}}^{\textbf{Identified model: } DSR_8^8}$$
$$B = \begin{bmatrix} 0.0233 \\ 0.0968 \\ -0.0664 \\ 0.0193 \end{bmatrix}, \quad D = \begin{bmatrix} -0.2129 & 0.5148 & 0.5587 & -0.4677 \end{bmatrix}, \quad K = \begin{bmatrix} -1.4571 \\ 4.2669 \\ -0.5973 \\ 0.5184 \end{bmatrix}. \tag{18}$$

We identified a similar 4th order model from the PEM algorithm, Tab. 3 shows how closely related these models are. Both models were compared over the validation set (Fig. 16), where dsr had the lowest prediction error, $V_{DSR} = 0.3932$.

Table 3: Comparing models identified from dsr and pem.

Algorithm	V_{MSE}	H_d	abs(eig(A))
DSR	0.3932	-0.0265	1.0000 1.0000 0.9891 0.9891
PEM	0.5039	-0.0270	1.0000 1.0000 0.9986 0.9986

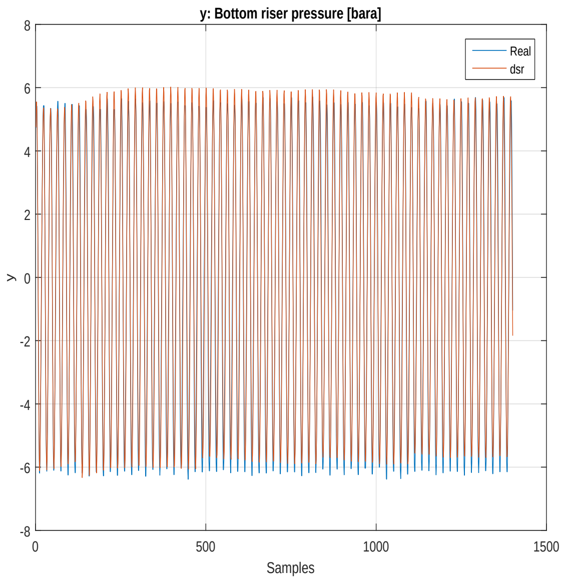

Figure 14: Illustration of the identified model DSR_8^8 in Eq. (18) simulated over the identification set resulting in $V_{MSE} = 0.3753$.

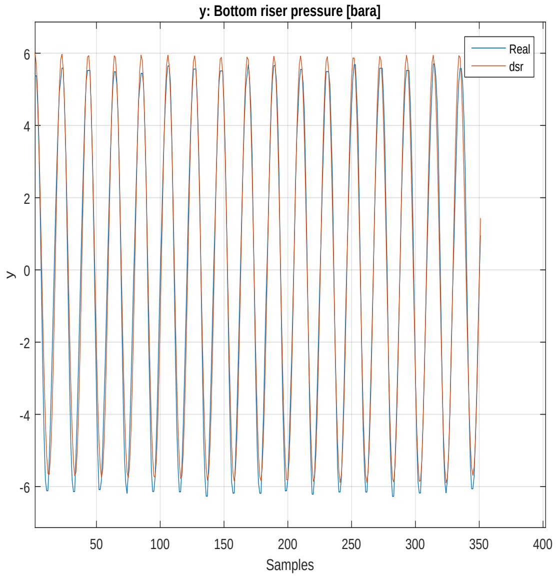

Figure 15: Identified model DSR_8^8 (Eq. 18) simulated over the identification set. This figure shows simulation from 500 to 850 samples in Fig. 14.

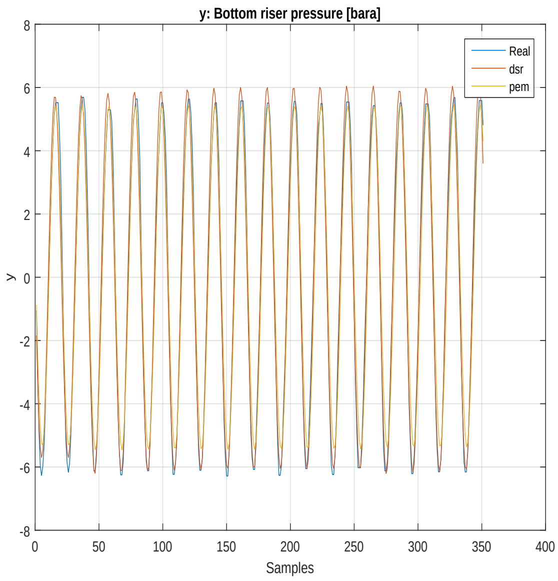

Figure 16: Illustration of the identified models simulated over the unused part of the validation set. We have $V_{DSR_8^8} = 0.3932$ $V_{PEM} = 0.5039$. See Fig. 13. for details.

Specified constrains:

$$u_k^{max} = 55, u_k^{min} = 15$$
$$\Delta u_k^{max} = 10, \Delta u_k^{min} = -10$$

An implementation of the MPC on the K-Spice/LedaFlow simulator is shown in Fig. 17. A prediction horizon, $L = 20$, and the following weights were chosen; $Q = 20$ and $R = 1$ based on simulation on the identified model.

It can be seen that both the controllers; MPC and LQR have successfully stabilized the undesired oscillating flow, up to 52 % choke opening, but the production/outlet flow remains constant at 42.9 $[kg/s]$. Both strategies also have quite similar performances, the difference is that the MPC is predictive, as illustrated in Fig. 19.

The LQR matrices G_1 and G_2 in $u_k = u_{k-1} + G_1 \Delta \bar{x}_k + G_2(y_{k-1} - r_k)$ are as in Eq. (19).

$$G_1 = \overbrace{\begin{bmatrix} -5.9951 & -4.2162 & 4.8841 & 16.6625 \end{bmatrix}}^{\textbf{LQ-optimal feedback matrices}}, \quad G_2 = \begin{bmatrix} 2.3356 \end{bmatrix}. \tag{19}$$

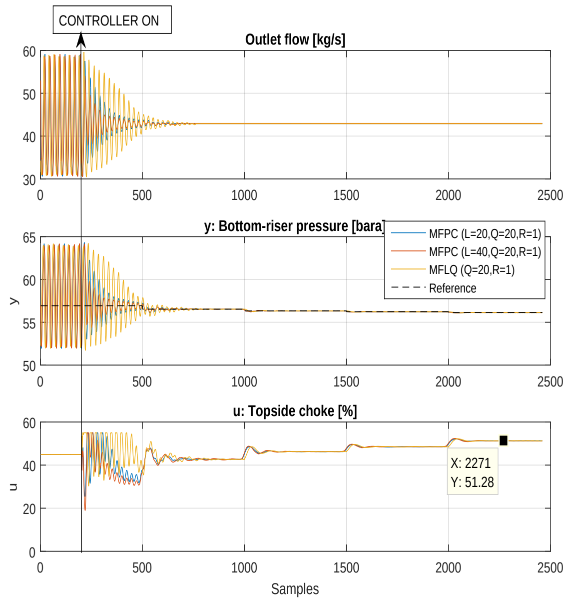

Figure 17: Implementation of MFPC and MFLQR on the K-Spice/LedaFlow simulator. Stabilizing up to 51.3 % choke opening. Simulation speed is 50 times real time. Sampling time is 1 sec.

4. Discussion and summary

Two examples are demonstrating the MFPC on the Di Meglio model and the K-Spice/LedaFlow simulator, where

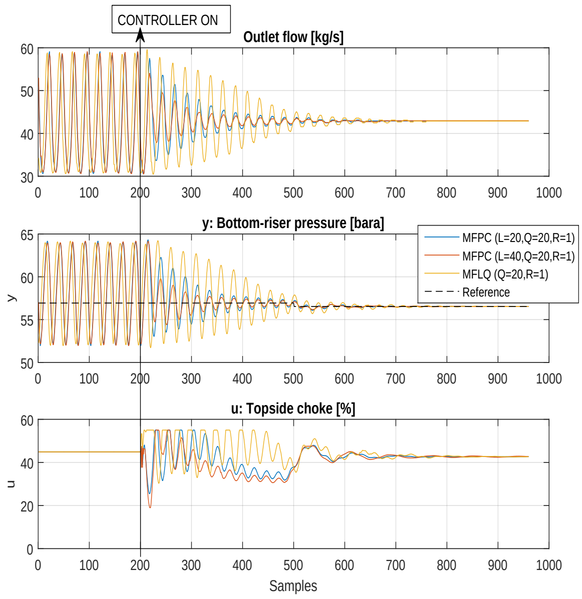

Figure 18: Comparing MFPC to MFLQR using the samples from 1 to 960 in Fig. 17.

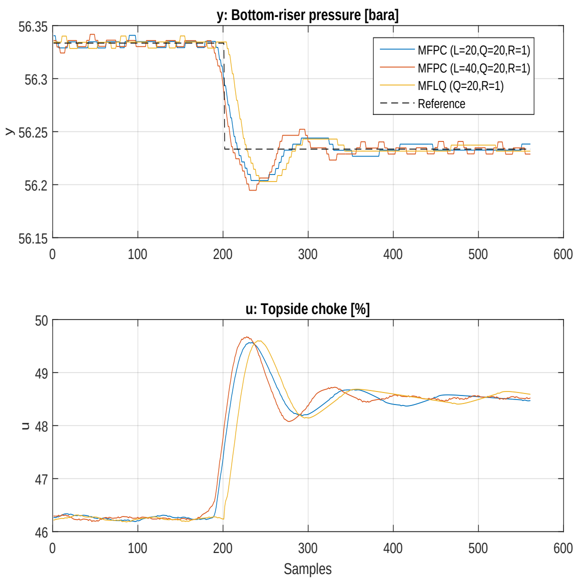

Figure 19: Comparing MFPC to MFLQR using the samples from 1300 to 1860 in Fig. 17.

Table 4: Comparing MFPC vs MFLQ using performance measures: Integrated Absolute Error (IAE) and Total Value (TV). Associated with Fig. 17.

Controller	Tuning parameters	IAE	TV
LQR	$Q = 10, R = 1$	856.0	796.4
MPC	$L = 20, Q = 10, R = 1$	450.0	368.3
MPC	$L = 40, Q = 10, R = 1$	312.4	327.8

the goal was to stabilize the outlet flow/bottom riser pressure at highest possible choke opening.

For the Di Meglio model we have that the MPFC, based @0.20 (marginally stable is defined at 0.205), was able to stabilize up to 0.39, while the other one, based @0.15, achieved 0.37. The runner-up candidate, i.e. the MFLQR, did only differ from the MFPC in terms of performance indices TV and IAE. Note that the PI controller could probably be tuned better for this case.

For the K-Spice/LedaFlow simulator we based the MFPC around a marginally stable working point, i.e. @44.9 %, and it was able to stabilize up to 52%.

5. Concluding Remarks

Practical implementation of MFPC was successfully demonstrated on a well-pipeline-riser process described by a 3-state non-linear model, thereafter it was demonstrated on the K-Spice/LedaFlow simulator.

Acknowledgment

The authors acknowledge in bullets

- Kongsberg Oil & Gas Technologies for supporting with license and software for the K-Spice and LedaFlow simulator.
- Telemark University College

MATLAB functions

The MATLAB functions used in this work are available for academic use upon request.

A. Complete model

The Di Meglio model may be formulated as a continues non-linear state space model, as

$$\begin{aligned} \dot{x} &= f(x, u), \\ y &= g(x), \end{aligned} \tag{20}$$

where

$$x = \begin{bmatrix} x_1 \\ x_2 \\ x_3 \end{bmatrix} = \begin{bmatrix} m_{g,cb} \\ m_{g,r} \\ m_{l,r} \end{bmatrix}, \quad f = \begin{bmatrix} f_1 \\ f_2 \\ f_3 \end{bmatrix}. \tag{21}$$

$$\begin{aligned} f_1 &= (1-\lambda)w_{g_0,in} - C_g max\Bigg(0, x_1 \frac{RT}{MV_{eb}} \\ &- \frac{x_2 RT}{M(V_r - (x_3 + m_{l,still})\rho_l)} \\ &- (x_3 + m_{l,still})\frac{gsin(\theta)}{A}\Bigg), \\ f_2 &= \lambda w_{g,in} + C_g max\Bigg(0, \frac{RT}{MV_{eb}} \\ &- \frac{x_2 RT}{M(V_r - (x_3 + m_{l,still})\rho_l)} \\ &- (x_3 + m_{l,still}\frac{gsin(\theta)}{A}\Bigg) \\ &- C_c u\left(\sqrt{\rho_l(\frac{x_2 RT}{M(V_r - (x_3 + m_{l,still})\rho_l)} - P_s)}\right)\frac{x_2}{x_3}, \\ f_3 &= w_{l,in} \\ &- C_c u\sqrt{\rho_l(\frac{x_2 RT}{M(V_r - (x_3 + m_{l,still})\rho_l)} - P_s)}, \\ g &= \frac{x_2 RT}{M(V_r - (x_3 + m_{l,still})\rho_l)} \\ &+ (x_3 + m_{l,still})\frac{g_0 sin(\theta)}{A10^5}. \end{aligned} \tag{22}$$

Table 5: Initial values for the simulations on Di Meglio model. The ODE is solved each timestep with MATLAB ode15s (sampling time, $\Delta t = 100$ sec.)

Variable	Value	Unit
x_0	$1.0e+03 \begin{bmatrix} 5.9075 \\ 0.3177 \\ 3.3867 \end{bmatrix}$	kg/s
y_0	y_m	bar
u_0	u_m	1

Table 6: Parameters for the Di Meglio model Eqs. 22.

Variable	Value	Unit
A	1.77E-2	m^2
θ	$\frac{\pi}{4}$	rad
ρ_l	900	$\frac{kg}{m^3}$
R	8.314	$\frac{J}{molK}$
T	363	K
P_s	6.6E5	$\frac{N}{m^2}$
$m_{l,still}$	3.73E4	kg
M	2.2E-2	$\frac{kg}{mol}$
λ	0.78	
L	5200	m
g_0	9.81	$\frac{m}{s^2}$
C_c	1E-4	ms
C_g	2.8E-3	m^2
$w_{l,in}$	11.75	$\frac{kg}{s}$
$w_{g,in}$	8.2E-1	$\frac{kg}{s}$
V_r	92.04	m^3
$V_{g,eb}$	48	m^3

References

Akaike, H. A new look at the statistical model identification. *Automatic Control, IEEE Transactions on*, 1974. 19(6):716–723. doi:10.1109/TAC.1974.1100705.

Courbot, A. Prevention of Severe Slugging in the Dunbar 16' Multiphase Pipeline. *Proc. Annual Offshore Technology Conference*, 1996. doi:10.4043/8196-MS.

Dalen, C., Di Ruscio, D., and Nilsen, R. Model-free optimal anti-slug control of a well-pipeline-riser in the K-Spice/LedaFlow simulator. *Modeling, Identification and Control*, 2015. 36(3):179–188. doi:10.4173/mic.2015.3.5.

Di Meglio, F., Kaasa, G., Petit, N., and Alstad, V. Model-based control of slugging flow: An experimental case study. In *American Control Conference (ACC), 2010*. pages 2995–3002, 2010a. doi:10.1109/ACC.2010.5531271.

Di Meglio, F., Kaasa, G.-O., and Petit, N. A first principle model for multiphase slugging flow in vertical risers. In *Decision and Control, 2009 held jointly with the 2009 28th Chinese Control Conference. CDC/CCC 2009. Proceedings of the 48th IEEE Conference on*. pages 8244–8251, 2009. doi:10.1109/CDC.2009.5400680.

Di Meglio, F., Kaasa, G.-O., Petit, N., and Alstad, V. Reproducing slugging oscillations of a real oil well. In *Decision and Control (CDC), 2010 49th IEEE Conference on*. pages 4473–4479, 2010b. doi:10.1109/CDC.2010.5717367.

Di Ruscio, D. Combined Deterministic and Stochastic System Identification and Realization: DSR - A Subspace Approach Based on Observations. *Modeling, Identification and Control*, 1996. 17(3):193–230. doi:10.4173/mic.1996.3.3.

Di Ruscio, D. Model Predictive Control with Integral Action: A simple MPC algorithm. *Model-*

ing, Identification and Control, 2013. 34(3):119–129. doi:10.4173/mic.2013.3.2.

Favoreel, W., Moor, B. D., Gevers, M., and Overschee, P. V. Closed-loop model-free subspace-based LQG-design. *in Proc. of the 7th Mediteranean Conference on Control and Automation (MED99), Haifa, Isreal*, 1999. pages 1926 – 1939. URL ftp://ftp.esat.kuleuven.be/pub/sista/ida/reports/98-107.pdf.

Godhavn, J.-M., Fard, M. P., and Fuchs, P. H. New slug control strategies, tuning rules and experimental results. *Journal of Process Control*, 2005. 15(5):547 – 557. doi:http://dx.doi.org/10.1016/j.jprocont.2004.10.003.

Jahanshahi, E. and Skogestad, S. Simplified dynamical models for control of severe slugging in multiphase risers. *18th IFAC World Congress*, 2013. 36(3):233–240. doi:10.3182/20110828-6-IT-1002.00981.

Jahanshahi, E. and Skogestad, S. Anti-slug control solutions based on identified model. *Journal of Process Control*, 2015. 30(0):58 – 68. doi:10.1016/j.jprocont.2014.12.007. CAB/DYCOPS 2013 Selected Papers From Two Joint {IFAC} Conferences: 9th International Symposium on Dynamics and Control of Process Systems and the 11th International Symposium on Computer Applications in Biotechnology, Leuven, Belgium, July 5-9, 2010.

K-Spice. K-Spice version 3.2. 2015. URL kongsberg.com/k-spice.

LedaFlow. LedaFlow version 1.7. 2015. URL kongsberg.com/ledaflow.

Ljung, L. System identification toolbox for use with {MATLAB}. 2007.

Ogazi AI, Y. H. . L. L., Cao Y. Slug control with large valve openings to maximize oil production. *SPE Journal*, 2010. 15(3):812–821. doi:10.2118/124883-PA.

Schmidt Z., J. P. . B., Brill. Choking can eliminate severe pipeline slugging. *Oil & Gas J*, 1979. 312:230–238.

Storkaas, E. and Skogestad, S. Cascade control of unstable systems with application to stabilization of slug flow. *AdChem, Hong Kong*, 2003a.

Storkaas, E. and Skogestad, S. A low-dimensional dynamic model of severe slugging for control design and analysis. 2003b. 11th International Conference on Multiphase flow (Multiphase '03).